Phenomenology of a Light Cold Dark Matter Two-Singlet Model

Abdessamad Abada[a,b*] and Salah Nasri[b†]

[a] *Laboratoire de Physique des Particules et Physique Statistique,*
Ecole Normale Supérieure, BP 92 Vieux Kouba, 16050 Alger, Algeria

[b] *Physics Department, United Arab Emirates University,*
POB 17551, Al Ain, United Arab Emirates

(Dated: January 9, 2012)

Abstract

We study the implications of phenomenological processes on a two-singlet extension of the Standard Model we introduced in a previous work to describe light cold dark matter. We look into the rare decays of Υ and B mesons, most particularly the invisible channels, and study the decay channels of the Higgs particle. Preferred regions of the parameter space are indicated, together with others that are excluded. Comments in relation to recent Higgs searches and finds at the LHC are made.

PACS numbers: 95.35.+d; 98.80.-k; 12.15.-y; 11.30.Qc.

Keywords: cold dark matter. light WIMP. extension of Standard Model.

*Electronic address: a.abada@uaeu.ac.ae

†Electronic address: snasri@uaeu.ac.ae

I. INTRODUCTION

While still elusive, dark matter is believed to contribute about 23% to the energy budget of the Universe [1]. We know it should be massive, stable on cosmic time scales and nonrelativistic when it decouples from the thermal bath in order to be consistent with structure formation. Although its mass and spin are not yet known, masses in the range of $5 - 10$ GeV seem to be favored by the direct detection experiments CoGeNT [2], DAMA [3] and CRESST II [4].

A number of models have been proposed to try to explain the results of these experiments [5]. As it turns out, having a light dark-matter candidate in supersymmetric theories is quite challenging. For instance, in mSUGRA, the constraint from WMAP and the bound on the pseudo-scalar Higgs mass from LEP give $m_{\chi_1^0} \geq 50\text{GeV}$ [6]. Also, in the MSSM, a lightest supersymmetric particle with a mass around 10GeV and an elastic scattering cross-section off a nuclei as large as 10^{-41}cm^2 is needed in order to fit the CoGeNT data, which in turn requires a very large $\tan\beta$ and a relatively light CP-odd Higgs. However, such a choice of parameters leads to a sizable contribution to the branching ratios of some rare decays, which then disfavors the scenario of light neutralinos in the context of the MSSM [7] (see also [8]).

In a recent work [9], we proposed a two-singlet extension of the Standard Model as a simple model for light cold dark matter. Both scalar fields were $\mathbb{Z}_2$-symmetric, with one undergoing spontaneous symmetry breaking while the other remaining unbroken to ensure stability of the dark-matter candidate. We studied the behavior of the model, in particular the effects of the dark-matter relic-density constraint and the restrictions from experimental direct detection. We concluded that the model was capable of bearing a light dark-matter weakly-interacting massive particle (WIMP) in mass regions where other models may find difficulties. We should mention in passing that there are scenarios with unstable light Higgs-like particles that have been previously studied in certain extensions of the Standard Model, see for example [10]. There is also the possibility of having a light pseudo-scalar in the NMSSM, see for example [11].

The present work studies the effects and restrictions on the two-singlet model coming from particle phenomenology. A limited selection of low-energy processes has to be made, and we choose to look into the rare decays of Υ and B mesons. We limit ourselves to small dark-matter masses, in the range $0.1 - 10$ GeV. We also study the implications of the model

on the decay channels of the Higgs particle and make quick comments in relation to recent finds at the LHC.

The theory starts effectively with eight parameters [9]. The spontaneous breaking of the electroweak and $\mathbb{Z}_2$ symmetries introduces the two vacuum expectation values v and v_1 respectively. The value of v is fixed experimentally to be 246GeV and we take $v_1 = 100$GeV. Four of the parameters are the three physical masses m_0 (dark-matter singlet S_0), m_1 (the second singlet S_1) and m_h (Higgs h), plus the mixing angle θ between h and S_1. We let m_1 vary in the interval $0.1 - 10$ GeV and fix the Higgs mass to $m_h = 125$GeV [12, 13], except in the part about the Higgs decays where we let m_h vary in the interval $100 - 200$ GeV[1]. For the purpose of our discussions, it is sufficient to let θ vary in the interval $1^{\rm o} - 40^{\rm o}$. The last parameters are the two physical mutual coupling constants $\lambda_0^{(4)}$ (dark matter – Higgs) and $\eta_{01}^{(4)}$ (dark matter – S_1 particle). In fact, $\eta_{01}^{(4)}$ is not free as it is the smallest real and positive solution to the dark-matter relic density constraint [9], which is implemented systematically throughout this work. Thus we are left with four parameters, namely, m_0 , m_1, θ and $\lambda_0^{(4)}$. To ensure applicability of perturbation theory, the requirement $\eta_{01}^{(4)} < 1$ is also imposed throughout, as well as a choice of rather small values for $\lambda_0^{(4)}$.

II. UPSILON DECAYS

We start by looking at the constraints on the parameter space of the model coming from the decay of the meson Υ in the state nS $(n = 1, 3)$ into one photon γ and one particle S_1. For $m_1 \lesssim 8$GeV, the branching ratio for this process is given by the relation:

$$\mathrm{Br}\left(\Upsilon_{nS} \to \gamma + S_1\right) = \frac{G_F m_b^2 \sin^2\theta}{\sqrt{2}\pi\alpha}\, x_n \left(1 - \frac{4\alpha_s}{3\pi} f(x_n)\right) \mathrm{Br}^{(\mu)}\, \Theta\left(m_{\Upsilon_{nS}} - m_1\right). \qquad (2.1)$$

In this expression, $x_n \equiv \left(1 - m_1^2/m_{\Upsilon_{ns}}^2\right)$ with $m_{\Upsilon_{1(3)S}} = 9.46(10.355)$GeV the mass of $\Upsilon_{1(3)S}$, the branching ratio $\mathrm{Br}^{(\mu)} \equiv \mathrm{Br}\left(\Upsilon_{1(3)S} \to \mu^+\mu^-\right) = 2.48(2.18) \times 10^{-2}$ [15], α is the QED coupling constant, $\alpha_s = 0.184$ the QCD coupling constant at the scale $m_{\Upsilon_{nS}}$, the quantity G_F is the Fermi coupling constant and m_b the b quark mass [16]. The function $f(x)$ incorporates the effect of QCD radiative corrections given in [17].

[1] The exclusion mass range reported by the CMS and ATLAS Collaborations applies to the SM Higgs and can be weakened or evaded in models where the Higgs production and/or decay channels are suppressed [14]. We will comment on this possibility within our model in the last section.

However, a rough estimate of the lifetime of S_1 indicates that this latter is likely to decay inside a typical particle detector, which means we ought to take into account its most dominant decay products. We first have a process by which S_1 decays into a pair of pions, with a decay rate given by:

$$\begin{aligned}\Gamma\left(S_1 \to \pi\pi\right) \;=\; & \frac{G_F m_1}{4\sqrt{2}\pi}\sin^2\theta\left[\frac{m_1^2}{27}\left(1+\frac{11m_\pi^2}{2m_1^2}\right)^2\right. \\ & \times\left(1-\frac{4m_\pi^2}{m_1^2}\right)^{\frac{1}{2}}\Theta[(m_1-2m_\pi)\left(2m_K-m_1\right)] \\ & \left.+3\left(M_u^2+M_d^2\right)\left(1-\frac{4m_\pi^2}{m_1^2}\right)^{\frac{3}{2}}\Theta\left(m_1-2m_K\right)\right]. \end{aligned} \tag{2.2}$$

Here, m_π is the pion mass and m_K the kaon mass. Also, chiral perturbation theory is used below the kaon pair production threshold, and the MIT bag model above, with the dressed u and d quark masses $M_u = M_d = 0.05\text{GeV}$. Note that this rate includes all pions, charged and neutral. Above the $2m_K$ threshold, there is the production of both a pair of kaons and η particles. The decay rate for K production is:

$$\Gamma\left(S_1 \to KK\right) = \frac{9}{13}\frac{3G_F M_s^2 m_1}{4\sqrt{2}\pi}\sin^2\theta\left(1-\frac{4m_K^2}{m_1^2}\right)^{\frac{3}{2}}\Theta\left(m_1-2m_K\right). \tag{2.3}$$

In the above rate, $M_s = 0.45\text{GeV}$ is the s quark bag-mass [18, 19]. For η production, replace m_K by m_η and $\frac{9}{13}$ by $\frac{4}{13}$.

The particle S_1 decays also into c and b quarks (mainly c). Including the radiative QCD corrections, the corresponding decay rates are given by:

$$\Gamma(S_1 \to q\bar{q}) = \frac{3G_F\bar{m}_q^2 m_1}{4\sqrt{2}\pi}\sin^2\theta\left(1-\frac{4\bar{m}_q^2}{m_h^2}\right)^{\frac{3}{2}}\left(1+5.67\frac{\bar{\alpha}_s}{\pi}\right)\Theta\left(m_1-2\bar{m}_q\right). \tag{2.4}$$

The dressed quark mass $\bar{m}_q \equiv m_q(m_1)$ and the running strong coupling constant $\bar{\alpha}_s \equiv \alpha_s(m_1)$ are defined at the energy scale m_1 [20]. There is also a decay into a pair of gluons, with the rate:

$$\Gamma\left(S_1 \to gg\right) = \frac{G_F m_1^3\sin^2\theta}{12\sqrt{2}\pi}\left(\frac{\alpha_s'}{\pi}\right)^2\left[6-2\left(1-\frac{4m_\pi^2}{m_1^2}\right)^{\frac{3}{2}}-\left(1-\frac{4m_K^2}{m_1^2}\right)^{\frac{3}{2}}\right]\Theta\left(m_1-2m_\pi\right). \tag{2.5}$$

Here, $\alpha_s' = 0.47$ is the QCD coupling constant at the bag-model scale.

We then have the decay of S_1 into leptons, the corresponding rate given by:

$$\Gamma\left(S_1 \to \ell^+\ell^-\right) = \frac{G_F m_\ell^2 m_1}{4\sqrt{2}\pi}\sin^2\theta\left(1-\frac{4m_\ell^2}{m_1^2}\right)^{\frac{3}{2}}\Theta\left(m_1-2m_\ell\right), \tag{2.6}$$

where m_ℓ is the lepton mass. Finally, S_1 can decay into a pair of dark matter particles, with a decay rate:

$$\Gamma\left(S_1 \to S_0 S_0\right) = \frac{\left(\eta_{01}^{(3)}\right)^2}{32\pi m_1}\sqrt{1-\frac{4m_0^2}{m_1^2}}\Theta\left(m_1-2m_0\right). \tag{2.7}$$

The coupling constant $\eta_{01}^{(3)}$ is given in [9]. The branching ratio for Υ_{nS} decaying via S_1 into a photon plus X, where X represents any kinematically allowed final state, will be:

$$\mathrm{Br}\left(\Upsilon_{nS} \to \gamma + X\right) = \mathrm{Br}\left(\Upsilon_{nS} \to \gamma + S_1\right) \times \mathrm{Br}\left(S_1 \to X\right). \tag{2.8}$$

In particular, $X \equiv S_0 S_0$ corresponds to a decay into invisible particles.

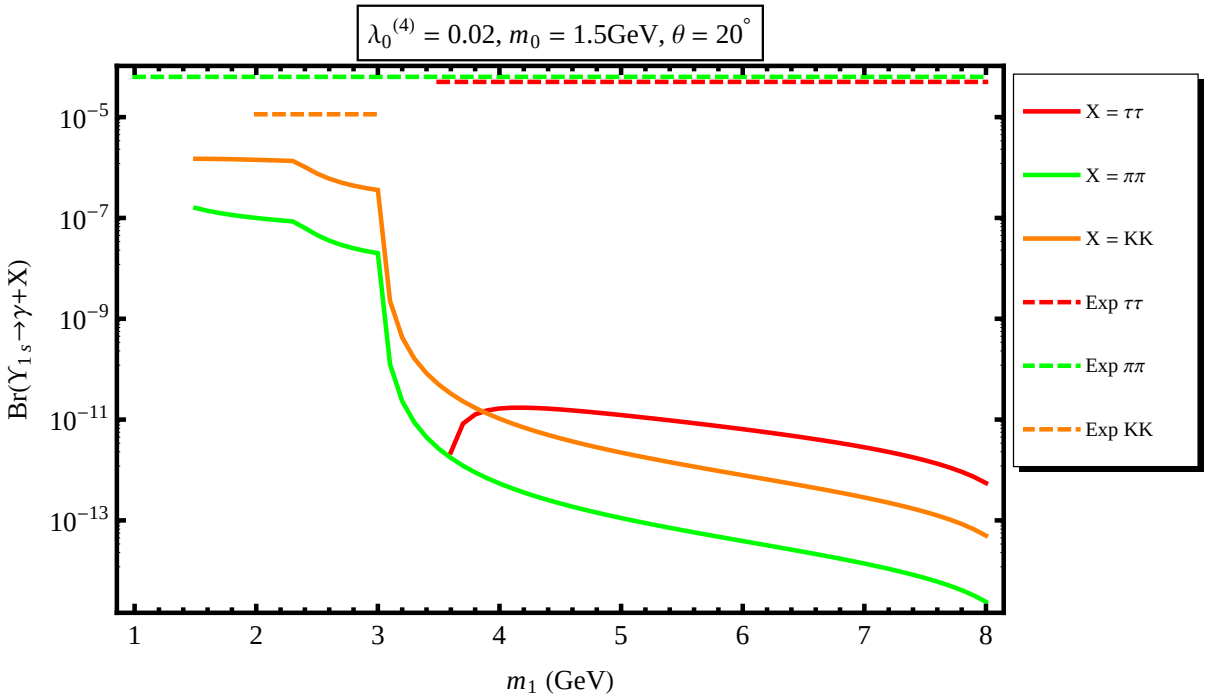

FIG. 1: Typical branching ratios of Υ_{1S} decaying into τ's, charged pions and charged kaons as functions of m_1. The corresponding experimental upper bounds are shown.

The best available experimental upper bounds on $1S$–state branching ratios are: (i) $\mathrm{Br}\left(\Upsilon_{1S} \to \gamma + \tau\tau\right) < 5 \times 10^{-5}$ for $3.5\mathrm{GeV} < m_1 < 9.2\mathrm{GeV}$ [21]; (ii) $\mathrm{Br}\left(\Upsilon_{1S} \to \gamma + \pi^+\pi^-\right) < 6.3 \times 10^{-5}$ for $1\mathrm{GeV} < m_1$ [22]; (iii) $\mathrm{Br}\left(\Upsilon_{1S} \to \gamma + K^+K^-\right) < 1.14 \times 10^{-5}$ for $2\mathrm{GeV} < m_1 < 3\mathrm{GeV}$ [23]. Figure 1 displays the corresponding branching ratios of Υ_{1S} decays via S_1 as functions of m_1, together with these upper bounds. Also, the best available experimental upper bounds on Υ_{3S} branching ratios are: (i) $\mathrm{Br}\left(\Upsilon_{3S} \to \gamma + \mu\mu\right) < 3 \times 10^{-6}$ for $1\mathrm{GeV} <$

$m_1 < 10\text{GeV}$; (ii) $\text{Br}\left(\Upsilon_{3S} \to \gamma + \text{Invisible}\right) < 3 \times 10^{-6}$ for $1\text{GeV} < m_1 < 7.8\text{GeV}$ [24]. Typical corresponding branching ratios are shown in figure 2.

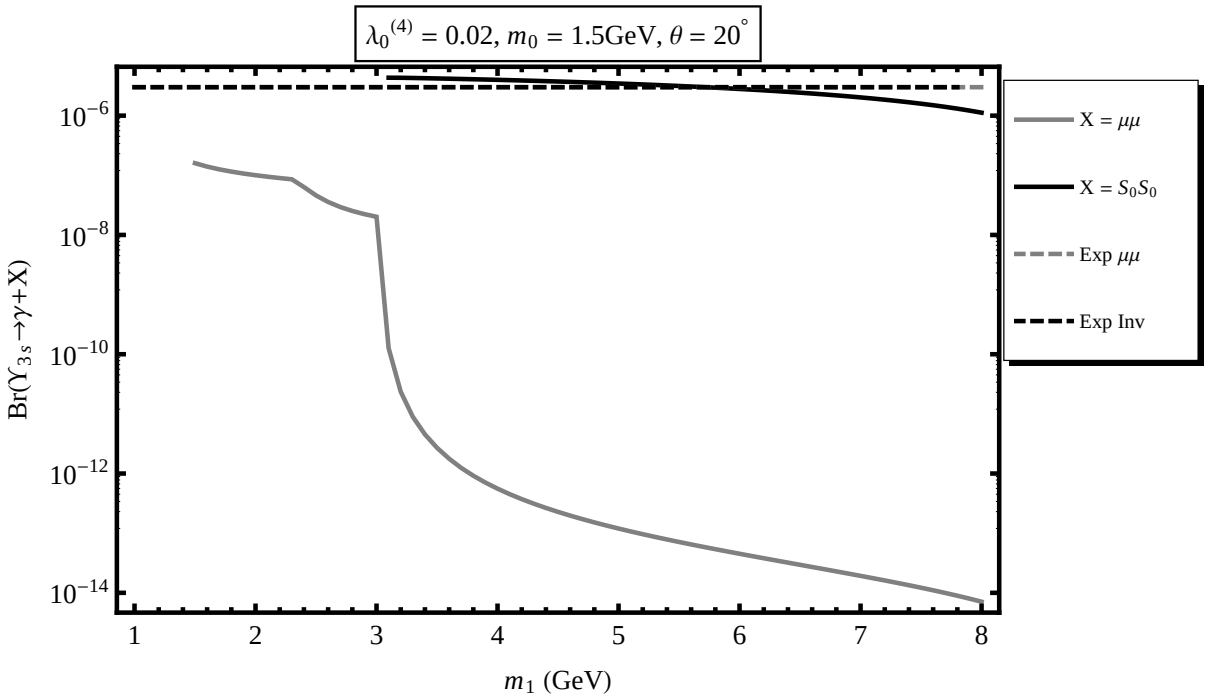

FIG. 2: Typical branching ratios of Υ_{3S} decaying into muons and dark matter as functions of m_1. The corresponding experimental upper bounds are shown.

A systematic scan of the parameter space indicates that the main effect of the Higgs-dark-matter coupling constant $\lambda_0^{(4)}$ and the dark-matter mass m_0 is to exclude, via the relic density and perturbativity constraints, regions of applicability of the model. This is shows in figures 1 and 2 where the region $m_1 \lesssim 1.4\text{GeV}$ is excluded. Otherwise, these two parameters have little effect on the shapes of the branching ratios themselves. The onset of the $S_0 S_0$ channel for $m_1 \geq 2m_0$ abates sharply the other channels and this one becomes dominant by far. The effect of the mixing angle θ is to enhance all branching ratios as it increases, due to the factor $\sin^2\theta$. The dark matter decay channel reaches the invisible upper bound already for $\theta \simeq 15^\circ$, for fairly small m_0, say 0.5GeV. The other channels find it hard to get to their respective experimental upper bounds, even for large values of θ.

III. B MESON DECAYS

Next we look at the flavor changing process in which the meson B^+ decays into a K^+ plus invisibles. The corresponding Standard-Model mode is a decay into K^+ and a pair of neutrinos, with a branching ratio $\mathrm{Br}^{\mathrm{SM}}\left(B^+ \to K^+ + \nu\bar{\nu}\right) \simeq 4.7{\times}10^{-6}$ [25]. The experimental upper bound is $\mathrm{Br}^{\mathrm{Exp}}\left(B^+ \to K^+ + \mathrm{Inv}\right) \simeq 14 \times 10^{-6}$ [26]. As in the Υ decays, the most prominent B invisible decay in this model is into $S_0 S_0$ via S_1 . The process $B^+ \to K^+ + S_1$ has a the branching ratio:

$$\begin{aligned}\mathrm{Br}\left(B^+ \to K^+ + S_1\right) \;=\; & \frac{9\sqrt{2}\tau_B G_F^3 m_t^4 m_b^2 m_+^2 m_-^2}{1024\pi^5 m_B^3 \left(m_b - m_s\right)^2} \left|V_{tb}V_{ts}^*\right|^2 f_0^2\left(m_1^2\right) \\ & \times\sqrt{\left(m_+^2 - m_1^2\right)\left(m_-^2 - m_1^2\right)}\, \sin^2\theta\, \Theta\left(m_- - m_1\right). \end{aligned} \tag{3.1}$$

Here $m_\pm = m_B \pm m_K$ where m_B is the B^+ mass, τ_B its lifetime, andV_{tb} and V_{ts} are flavor changing CKM coefficients. The function $f_0\left(s\right)$ is given by the relation:

$$f_0\left(s\right) = 0.33 \exp\left[\frac{0.63s}{m_B^2} - \frac{0.095s^2}{m_B^4} + \frac{0.591s^3}{m_B^6}\right]. \tag{3.2}$$

The different S_1 decay modes are given in (2.2) - (2.7) above. The branching ratio of B^+ decaying into $K^+ + S_0 S_0$ via the production and propagation of an intermediary S_1 will be:

$$\mathrm{Br}^{(S_1)}\left(B^+ \to K^+ + S_0 S_0\right) = \mathrm{Br}\left(B^+ \to K^+ + S_1\right) \times \mathrm{Br}\left(S_1 \to S_0 S_0\right). \tag{3.3}$$

Figure 3 displays a typical behavior of $\mathrm{Br}^{(S_1)}\left(B^+ \to K^+ + S_0 S_0\right)$ as a function of m_1. The branching ratio is well above the experimental upper bound, and θ as small as 1^{o} will not help with this, no matter what the values for $\lambda_0^{(4)}$ and m_0 are. So, for $m_1 \lesssim 4.8\mathrm{GeV}$, this process excludes the two-singlet model for $m_0 < m_1/2$. For $m_1 \gtrsim 4.8\mathrm{GeV}$ or $m_0 \geq m_1/2$, the decay does not occur, so no constraints on the model from this process.

Another process involving B mesons is the decay of B_s into predominately a pair of muons. The Standard Model branching ratio for this process is $\mathrm{Br}^{\mathrm{SM}}\left(B_s \to \mu^+\mu^-\right) = (3.2 \pm 0.2) \times 10^{-9}$ [27], and the experimental upper bound is $\mathrm{Br}^{\mathrm{Exp}}\left(B_s \to \mu^+\mu^-\right) < 1.08 \times 10^{-8}$ [28]. In the present model, two additional decay diagrams occur, both via intermediary S_1, yielding together the branching ratio:

$$\mathrm{Br}^{(S_1)}(B_s \to \mu^+\mu^-) = \frac{9\tau_{B_s} G_F^4 f_{B_s}^2 m_{B_s}^5}{2048\pi^5} m_\mu^2 m_t^4 \left|V_{tb}V_{ts}^*\right|^2 \frac{\left(1 - 4m_\mu^2/m_{B_s}^2\right)^{3/2}}{\left(m_{B_s}^2 - m_1^2\right)^2 + m_1^2\Gamma_1^2} \sin^4\theta. \tag{3.4}$$

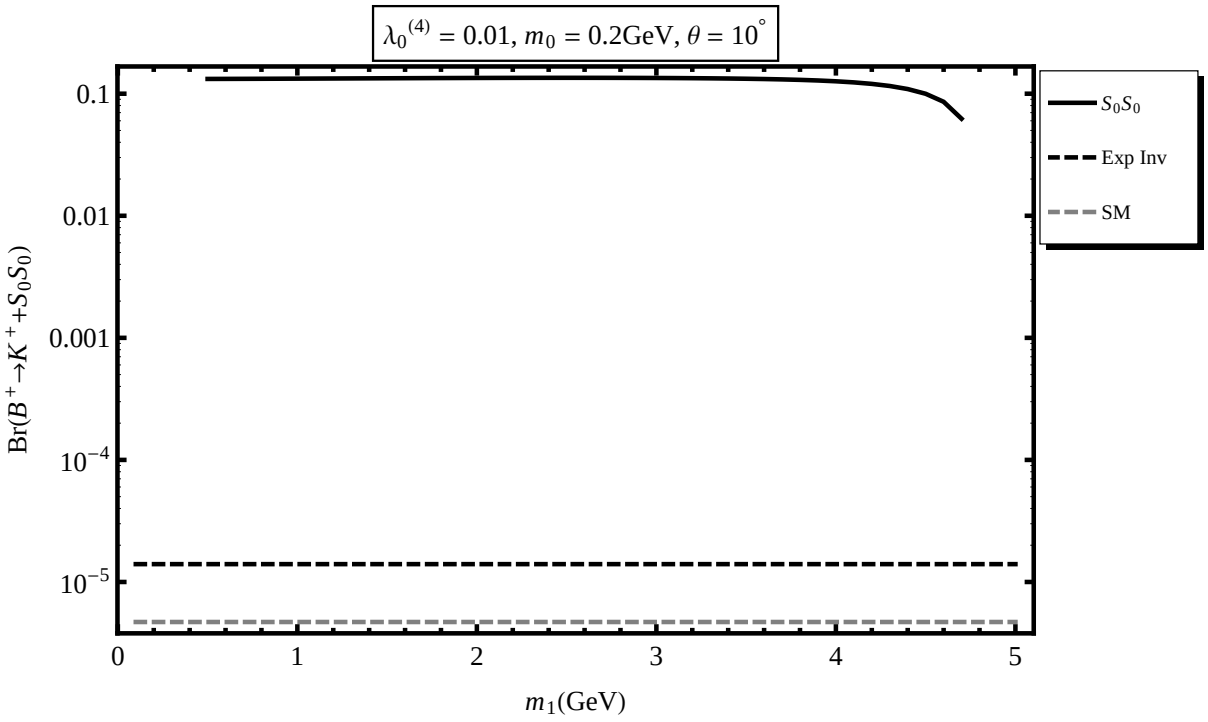

FIG. 3: Typical branching ratio of B^+ decaying into dark matter via S_1 as a function of m_1. The SM and experimental bounds are shown.

In this relation, τ_{B_s} is the B_s life-time, $m_{B_s} = 5.37$GeV its mass, and f_{B_s} a form factor that we take equal to 0.21GeV. The quantity Γ_1 is the total width of the particle S_1 [9].

A typical behavior of $\mathrm{Br}^{(S_1)}(B_s \to \mu^+\mu^-)$ as a function of m_1 is shown in figure 4. The peak is at m_{B_s}. All three parameters $\lambda_0^{(4)}$, m_0 and θ combine in the relic density constraint to exclude regions of applicability of the model. For example, for the values of figure 4, the region $m_1 < 2.2$ GeV is excluded. However, a systematic scan of the parameter space shows that outside the relic density constraint, $\lambda_0^{(4)}$ has no significant direct effect on the shape of $\mathrm{Br}^{(S_1)}(B_s \to \mu^+\mu^-)$. As m_0 increases, it sharpens the peak of the curve while pushing it up. This works until about 2.7GeV, beyond which m_0 ceases to have any significant direct effect. Increasing θ enhances the values of the branching ratio without affecting the width.

Also, for all the range of m_1, all of $\mathrm{Br}^{(S_1)} + \mathrm{Br}^{\mathrm{SM}}$ stays below $\mathrm{Br}^{\mathrm{Exp}}$ as long as $\theta < 10^{\mathrm{o}}$. As θ increases beyond this value, the peak region pushes up increasingly above $\mathrm{Br}^{\mathrm{Exp}}$ and thus gets excluded. Hoping for a clear signal if any, figure 5 displays a density plot showing $\mathrm{Br}^{\mathrm{SM}}+\mathrm{Br}^{(S_1)}(B_s \to \mu^+\mu^-)$ in the plane (m_1, θ), squeezed between $\mathrm{Br}^{\mathrm{SM}}+5\sigma$ from below and $\mathrm{Br}^{\mathrm{Exp}}$ from above. The behavior we see in this figure is generic across the ranges of m_0 and

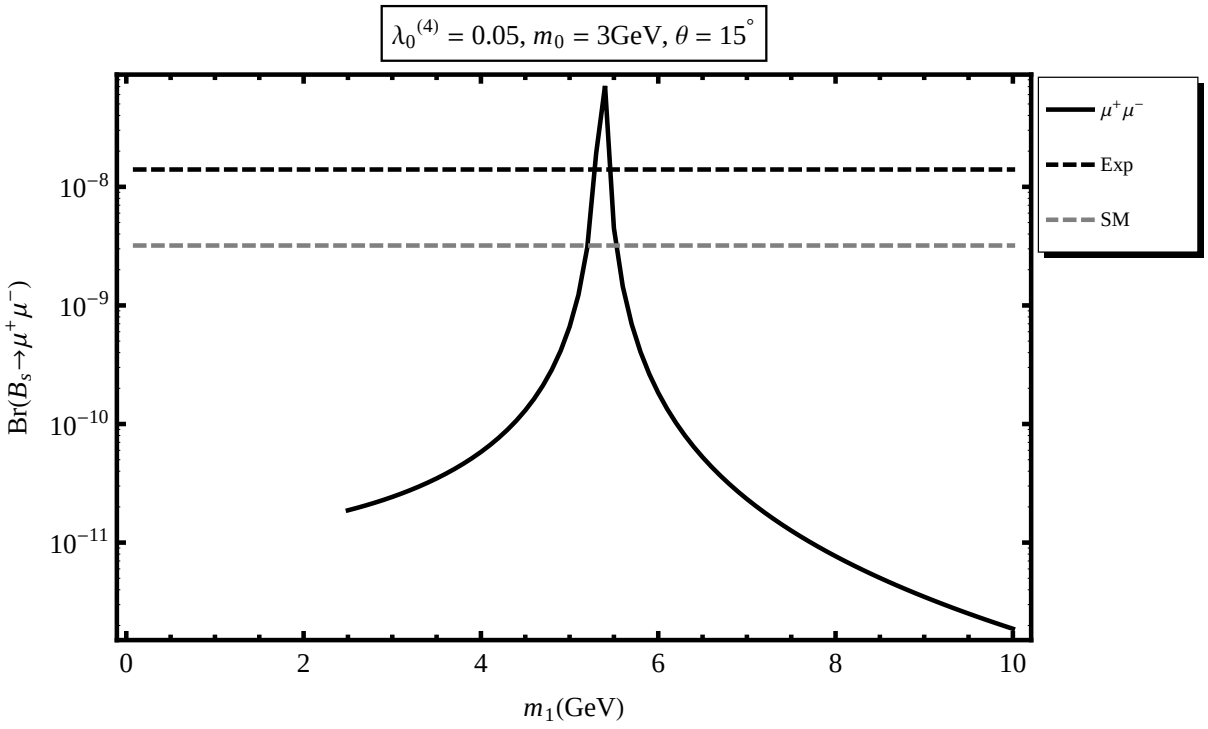

FIG. 4: Typical behavior of $\text{Br}^{(S_1)}(B_s \to \mu^+\mu^-)$ as a function of m_1, together with the SM and experimental bounds.

$\lambda_0^{(4)}$: the V-shape structure in gray developing from $m_1 = m_{B_s}$ is the allowed region. The white region in the middle is due to Br^{Exp}, and the white region outside to $\text{Br}^{\text{SM}} + 5\sigma$. It can happen that some of the gray V is eaten up by the relic-density constraint and perturbativity requirement for larger values of $\lambda_0^{(4)}$.

From this process, there is probably one element to retain if we want the model to contribute a distinct signal to $B_s \to \mu^+\mu^-$ for the range of m_0 chosen, and that is to restrict $4\text{GeV} \lesssim m_1 \lesssim 6.5\text{GeV}$. No additional constraint on m_0 is necessary while keeping $\lambda_0^{(4)} \lesssim 0.1$ to avoid systematic exclusion from direct detection is safe.

IV. HIGGS DECAYS

We finally examine the implications of the model on the Higgs different decay modes. In this part of the work, we allow the Higgs mass m_h to vary in the interval $100\text{GeV} - 200\text{GeV}$. First, h can decay into a pair of leptons ℓ, predominantly τ's. The corresponding decay rate $\Gamma(h \to \ell^+\ell^-)$ is given by the relation (2.6) where we replace m_1 by m_h . It can also

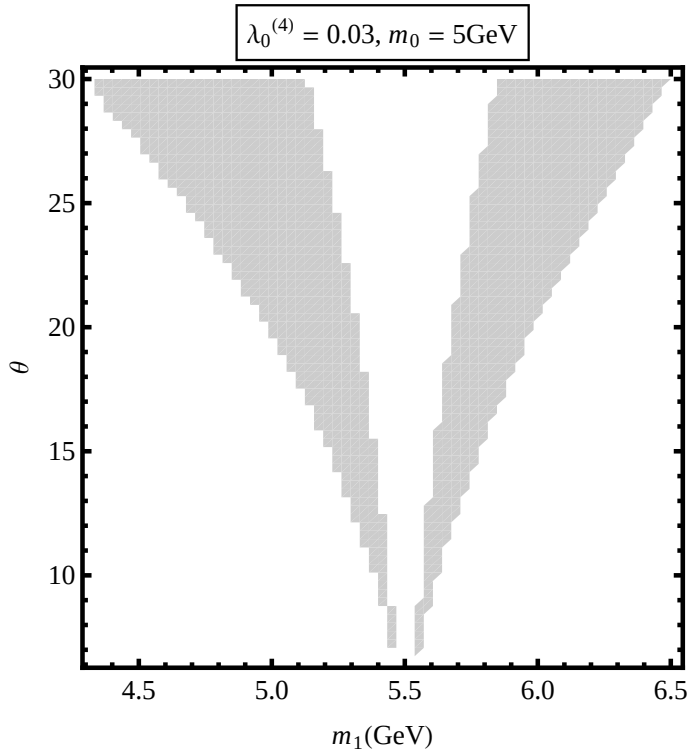

FIG. 5: A density plot of $B^{\rm SM} + {\rm Br}^{(S_1)}$ squeezed between $B^{\rm SM} + 5\sigma$ from below and $B^{\rm Exp}$ from above.

decay into a pair of quarks q, mainly into b's and, to a lesser degree, into c's. Here too the decay rate $\Gamma(h \to q\bar{q})$ is given in (2.4) with the replacement m_h instead of m_1. Then the Higgs can decay into a pair of gluons. Including the next-to-next-to-leading QCD radiative corrections, the corresponding decay rate can write like this:

$$\begin{aligned}\Gamma\left(h \to gg\right) \;=\; & \frac{G_F m_h^3}{4\sqrt{2}\pi}\left|\sum_q \frac{m_q^2}{m_h^2}\int_0^1 dx \int_0^{1-x} dy \frac{1-4xy}{\frac{m_q^2}{m_h^2} - xy}\right|^2 \\ & \times \left(\frac{\bar{\alpha}_s}{\pi}\right)^2 \left[1 + \frac{215}{12}\frac{\bar{\alpha}_s}{\pi} + \frac{\bar{\alpha}_s^2}{\pi^2}\left(156.8 - 5.7\log\frac{m_t^2}{m_h^2}\right)\right]\cos^2\theta, \end{aligned} \tag{4.1}$$

where the sum is over all quark flavors q. A systematic study of the double integral above shows that, with m_h in the range 100GeV – 200GeV, the t quark dominates in the sum over q, with non-negligible contributions from the c and b quarks.

For m_h smaller than the W or Z pair-production threshold, the Higgs can decay into a pair of one real and one virtual gauge bosons, with rates given by:

$$\Gamma\left(h \to VV^*\right) = \frac{3G_F^2 m_V^4 m_h}{16\pi^3}\cos^2\theta\, A_V\, R\left(\frac{m_V^2}{m_h^2}\right)\Theta\left[\left(m_h - m_V\right)\left(2m_V - m_h\right)\right]. \tag{4.2}$$

In this expression, m_V is the mass of the gauge boson V, the factor $A_V = 1$ for W and $\left(\frac{7}{12} - \frac{10}{9}\sin^2\theta_w + \frac{40}{9}\sin^4\theta_w\right)$ for Z with θ_w the Weinberg angle, and we have:

$$\begin{aligned} R(x) \;=\; & \frac{3(1-8x+20x^2)}{\sqrt{4x-1}}\arccos\left(\frac{3x-1}{2x^{3/2}}\right) \\ & -\frac{1-x}{2x}\left(2-13x+47x^2\right) - \frac{3}{2}\left(1-6x+4x^2\right)\log x. \end{aligned} \tag{4.3}$$

For a heavier Higgs particle, the decay rates into a V pair is given by:

$$\Gamma\left(h \to VV\right) = \frac{G_F m_V^4 \cos^2\theta}{\sqrt{2}\pi m_h} B_V \left(1 - \frac{4m_V^2}{m_h^2}\right)^{\frac{1}{2}} \left[1 + \frac{\left(m_h^2 - 2m_V^2\right)^2}{8m_V^4}\right] \Theta\left(m_h - 2m_V\right), \tag{4.4}$$

with $B_V = 1$ for W and $\frac{1}{2}$ for Z.

While all these decay modes already exist within the Standard Model, the two-singlet extension introduces two additional (invisible) modes, namely a decay into a pair of S_0's and a pair of S_1's. The corresponding decay rates are:

$$\Gamma\left(h \to S_i S_i\right) = \frac{\lambda_i^2}{32\pi m_h}\left(1 - \frac{4m_i^2}{m_h^2}\right)^{\frac{1}{2}} \Theta\left(m_h - 2m_i\right), \tag{4.5}$$

where $\lambda_i = \lambda_{0(2)}^{(3)}$ for $S_{0(1)}$ are coupling constants given in [9], functions of the parameters of the theory. The total decay rate $\Gamma\left(h\right)$ of the Higgs particle is the sum of these partial rates. The branching ratio corresponding to a particular decay will be $\mathrm{Br}\left(h \to X\right) = \Gamma\left(h \to X\right)/\Gamma\left(h\right)$.

Typical behaviors of the most prominent branching ratios are displayed in figure 6. A systematic study shows that for all ranges of the parameters, the Higgs decays dominantly into invisible. The production of fermions and gluons is comparatively marginal, whereas that of W and Z pairs takes relative importance towards and above the corresponding thresholds, and more significantly at larger values of the mixing angle θ.

However, the decay distribution between S_0 and S_1 is not even. The most dramatic effect comes from the coupling constant $\lambda_0^{(4)}$. When it is very small, the dominant production is that of a pair of S_1. This is exhibited in figure 6 for which $\lambda_0^{(4)} = 0.01$. As it increases, there is a gradual shift towards a more dominating dark-matter pair production, a shift competed against by an increase in θ. Figure 7 displays the branching ratios for $\lambda_0^{(4)} = 0.1$ and figure 8 for the larger value $\lambda_0^{(4)} = 0.7$. In general, increasing θ smoothens the crossings of the WW and ZZ thresholds, and lowers the production of everything except that of a pair of S_1, which is instead increased.

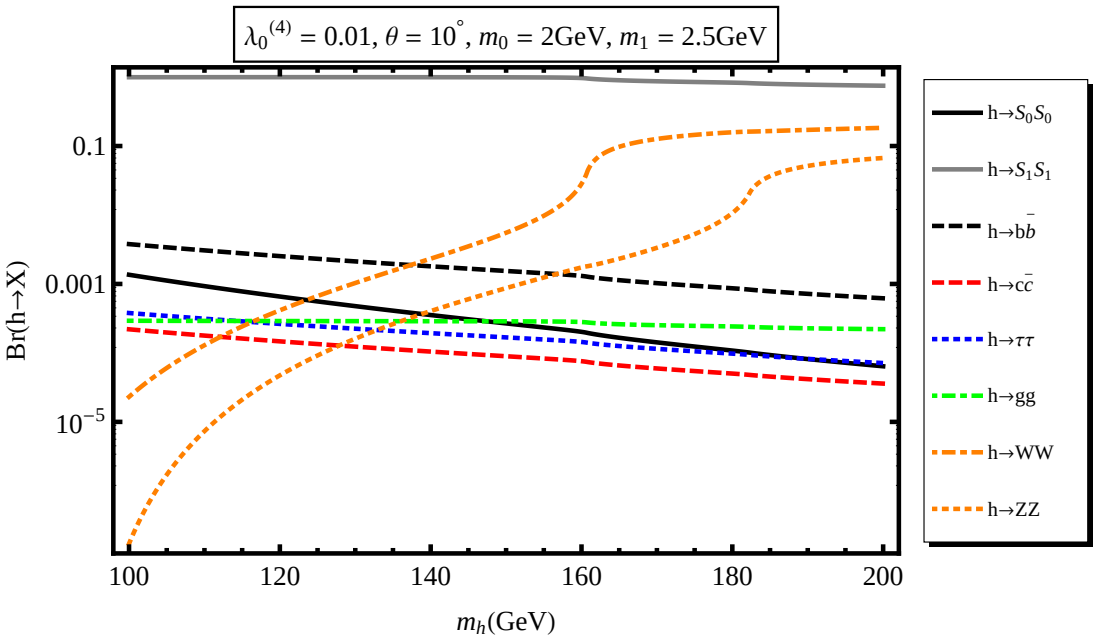

FIG. 6: Branching ratios for Higgs decays. Very small dark-matter Higgs coupling.

Like in the Standard Model, the production of a pair of b quarks dominates over the production of the other fermions, and all fermions are not favored by increasing $\lambda_0^{(4)}$. Changes in m_0 and m_1 have very little direct effects on all the branching ratios except that of S_0S_0 production where, at small θ, increasing m_1 (m_0) increases (decreases) the branching ratio, with reversed effects at larger θ. Note though that these masses have indirect impact through the relic density constraint by excluding certain regions [9].

V. CONCLUDING REMARKS

In this work, we have explored some phenomenological aspects of a two-singlet extension of the Standard Model we proposed as a simple model for light cold dark matter. We have looked into the rare decays of Υ and B mesons and studied the implications of the model on the decay channels of the Higgs particle.

For both Υ and B decays, apart from combining with the other two parameters in the relic-density and perturbativity constraints to exclude regions of applicability of the model, the Higgs-dark-matter coupling constant $\lambda_0^{(4)}$ and the dark-matter mass m_0 have little effect on the shapes of the branching ratios. Also, the effect of increasing the $h - S_1$ mixing

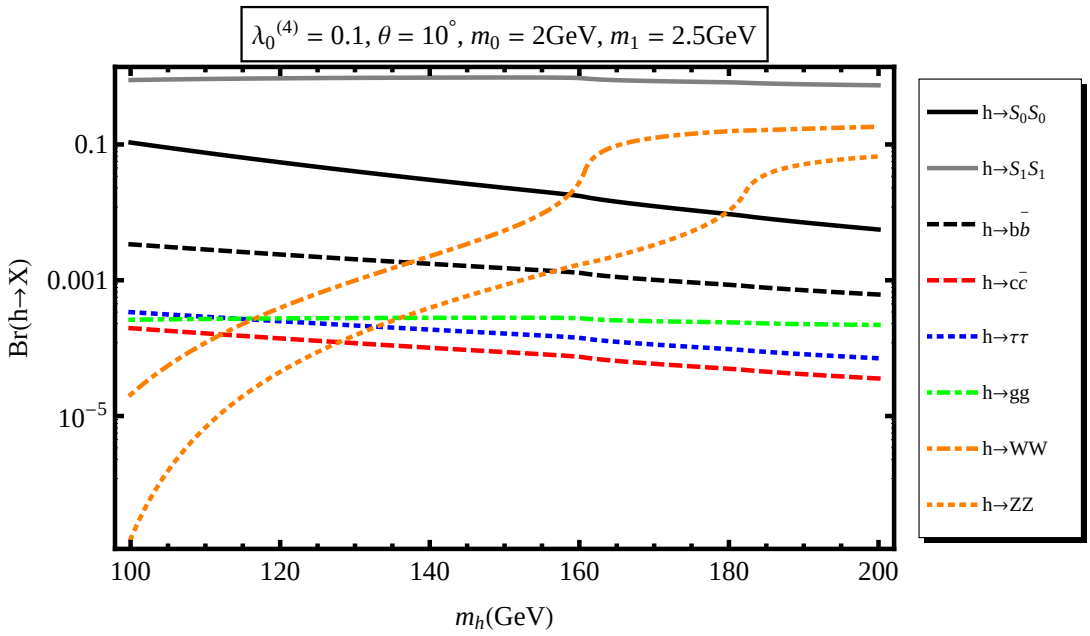

FIG. 7: Branching ratios for Higgs decays. Small dark-matter Higgs coupling.

angle θ is to enhance all branching ratios. For Υ decays, the dark-matter channel, when kinematically allowed ($m_1 \geq 2m_0$), dominates over the other decay modes. It reaches the experimental invisible upper bound for already fairly small values of θ and m_0. From B^+ decays, we learn that our model is excluded for $m_1 < 4.8\text{GeV}$ ($= m_B - m_K$) and $m_0 < m_1/2$. From B_s decay into muons, we learn that for the model to contribute a distinct signal to this process, it is best to restrict $4\text{GeV} \lesssim m_1 \lesssim 6.5\text{GeV}$ with no additional constraint on m_0. Also, in general, keeping $\lambda_0^{(4)} \lesssim 0.1$ to avoid systematic exclusion from direct detection for all these processes is safe.

Before closing this section, we comment on the effect that dark matter in our model has on Higgs searches. Since $m_h \gg 2m_0$, the process $h \to S_0 S_0$ is kinematically allowed and, for a large range of the parameter space, the ratio

$$\mathcal{R}^{(b)}_{\text{decay}} = \frac{\text{Br}\,(h \to S_0 S_0)}{\text{Br}(h \to b\bar{b})} \tag{5.1}$$

can be larger than one for $m_h < 120\text{GeV}$ as can be seen in figure 7. In this situation, the LEP bound on the Higgs mass can be weaker. Also, in our model, the Higgs production at LEP via Higgstrahlung can be smaller than the one in the Standard Model, and so the Higgs can be as light as 100GeV. Such a light Higgs would be in good agreement with the electroweak precision tests .

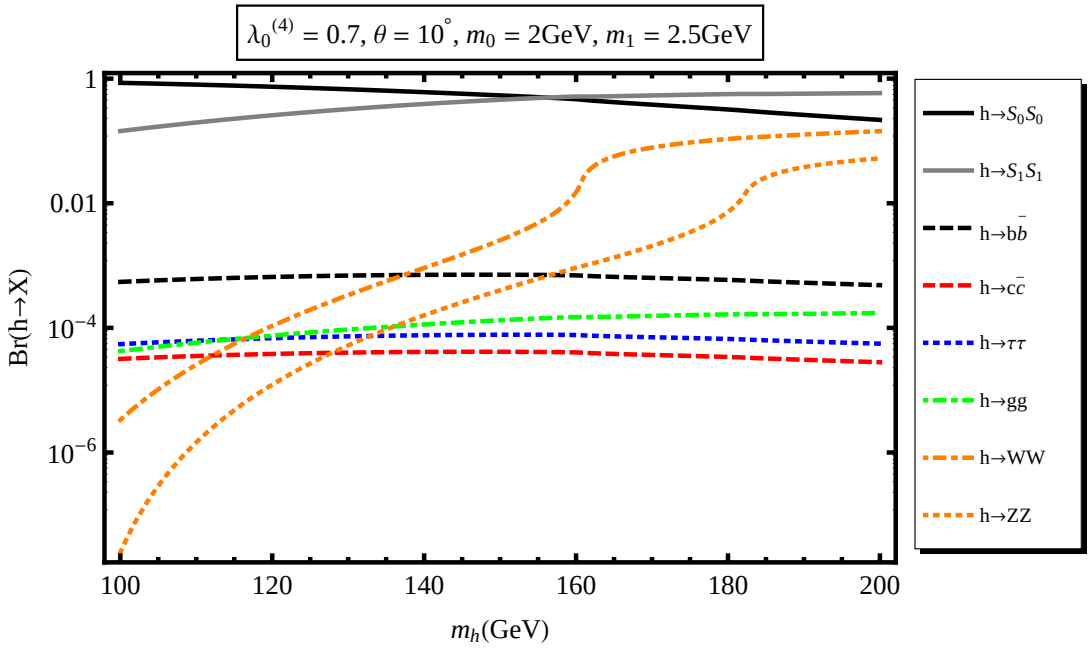

FIG. 8: Branching ratios for Higgs decays. Larger dark-matter Higgs coupling.

As to the Higgs searches at the LHC, the ATLAS and CMS collaborations have reported recently the exclusion of a Higgs mass in the interval 145 – 460 GeV [12, 13], which seems to suggest that we should have limited our analysis of the Higgs branching ratios to $m_h < 145$GeV. However, it is important to note that these experimental constraints apply to the SM Higgs and can not therefore be used as such if the Higgs interactions are modified. In our model, the mixing of h with S_1 will result in a reduction of the statistical significance of the Higgs discovery at the LHC. Indeed, the relevant quantity that allows one to use the experimental limits on Higgs searches to derive constraints on the parameters of the model is the ratio:

$$\mathcal{R}_{X_{\rm SM}} \equiv \frac{\sigma\left(gg\to h\right)\mathrm{Br}\left(h\to X_{\rm SM}\right)}{\sigma^{(\rm SM)}\left(gg\to h\right)\mathrm{Br}^{\rm SM}\left(h\to X_{\rm SM}\right)} = \frac{\cos^4\theta}{\cos^2\ \theta+\Gamma\left(h\to X_{\rm inv}\right)/\Gamma_h^{\rm SM}}. \qquad (5.2)$$

In this expression, $X_{\rm SM}$ corresponds to all the Standard Model particles, $X_{\rm inv} = S_0S_0$ and S_1S_1, σ is a cross-section, $\mathrm{Br}^{\rm SM}\left(h\to X\right)$ the branching fraction of the SM Higgs decaying into any kinematically allowed mode X, and $\Gamma_h^{\rm SM}$ the total Higgs decay rate in the Standard Model. To open up the region $m_h > 140$GeV requires the ratio $\mathcal{R}_{X_{\rm SM}}$ to be smaller than 0.25 [12, 13], a constraint easily fulfilled in our model. By comparison, the minimal extensions of the Standard Model with just one singlet scalar or a Majorana fermion, even under Z_2 symmetry, are highly constrained in this regard [29].

Beyond the present investigation, many other aspects of the model, partly in relation with the current LHC searches, are just waiting to be explored.

---

[1] J. Dunkley *et al.* [WMAP Collaboration], Astrophys. J. Suppl. **180**, 306 (2009) [arXiv:0803.0586 [astro-ph]].

[2] C. E. Aalseth *et al.* [CoGeNT collaboration], Phys. Rev. Lett. **107**, 141301 (2011) [arXiv:1106.0650 [astro-ph.CO]]; Phys. Rev. Lett. **106**, 131301 (2011) [arXiv:1002.4703 [astro-ph.CO]].

[3] R. Bernabei *et al.* [DAMA Collaboration], Eur. Phys. J. C **67**, 39 (2010) [arXiv:1002.1028 [astro-ph.GA]]; Eur. Phys. J. C **56**, 333 (2008) [arXiv:0804.2741 [astro-ph]].

[4] G. Angloher *et al.*, arXiv:1109.0702 [astro-ph.CO].

[5] Y. Mambrini, arXiv:1108.0671 [hep-ph]; Y. Kajiyama, H. Okada and T. Toma, arXiv:1109.2722 [hep-ph]; J. M. Cline and A. R. Frey, Phys. Rev. D **84**, 075003 (2011); R. Kappl, M. Ratz and M. W. Winkler, Phys. Lett. B **695**, 169 (2011); Y. Mambrini and B. Zaldivar, JCAP **1110**, 023 (2011); P. Draper, T. Liu, C. E. M. Wagner, L. T. M. Wang and H. Zhang, Phys. Rev. Lett. **106**, 121805 (2011); R. Foot, Phys. Lett. B **703**, 7 (2011); ; M. Gonderinger, Y. Li, H. Patel and M. J. Ramsey-Musolf, JHEP **053**, 1001 (2010); S. Andreas, C. Arina, T. Hambye, F. S. Ling and M. H. G. Tytgat, Phys. Rev. D **82**, 043522 (2010); K. J. Bae, H. D. Kim and S. Shin, Phys. Rev. D **82**, 115014 (2010); M. Farina, D. Pappadopulo and A. Strumia, Phys. Lett. B **688**, 329 (2010); V. Barger, P. Langacker, M. McCaskey, M. J. Ramsey-Musolf and G. Shaughnessy, Phys. Rev. **D77** 035005 (2008).

[6] Y. Akrami, P. Scott, J. Edsjo, J. Conrad and L. Bergstrom, JHEP **1004**, 057 (2010); G. Belanger, F. Boudjema, A. Pukhov and R. K. Singh, JHEP **0911**, 026 (2009).

[7] D. T. Cumberbatch, D. E. Lopez-Fogliani, L. Roszkowski, R. R. de Austri and Y. L. Tsai, arXiv:1107.1604 [astro-ph.CO]; D. A. Vasquez, G. Belanger, C. Boehm, A. Pukhov and J. Silk, Phys. Rev. D **82**, 115027 (2010); E. Kuflik, A. Pierce and K. M. Zurek, Phys. Rev. **D81** 111701 (2010); D. Feldman, Z. Liu and P. Nath, Phys. Rev. **D81** 117701 (2010).

[8] N. Fornengo, S. Scopel and A. Bottino, Phys. Rev. D **83**, 015001 (2011); V. Niro, A. Bottino, N. Fornengo and S. Scopel, Phys. Rev. **D80** 095019 (2009).

[9] A. Abada, D. Ghaffor and S. Nasri, Phys. Rev. **D83** 095021 (2011)

[arXiv:1101.0365[hep-ph]].

[10] K. J. Bae, H. D. Kim and S. Shin, Phys. Rev. D**82**, 115014 (2010).

[11] R. Dermisek and J. F. Gunion, Phys. Rev. D**81**, 075003 (2010).

[12] [ATLAS Collaboration], arXiv:1112.2577 [hep-ex]; G. Aad *et al.* [ATLAS Collaboration], Eur. Phys. J. C **71**, 1728 (2011).

[13] [CMS Collaboration], CMS-PAS-HIG-11-025, CMS-PAS-HIG-11-029, CMS-PAS-HIG-11-030, CMS-PAS-HIG-11-031, CMS-PAS-HIG- 11-032; S. Chatrchyan *et al.*, Phys. Lett. B **699**, 25 (2011).

[14] Y. Bai, J. Fan and J. L. Hewett, arXiv:1112.1964 [hep-ph].

[15] S. Eidelman *et al.*, Phys. Lett. B **592**, 1 (2004).

[16] K. Nakamura *et al.* (Particle Data Group), JP G **37**, 075021 (2010).

[17] P. Nason, Phys. Lett. B **175**, 223 (1986).

[18] J. F. Gunion, H. E. Haber, G. Kane and S. Dawson, ' *The Higgs Hunters Guide*' (Perseus Publishing, Cambridge, MA, 1990).

[19] D. McKeen, Phys. Rev. D **79**, 015007 (2009).

[20] A. Djouadi, Phys. Rept. **459**, 1 (2008).

[21] W. Love *et al.*, Phys. Rev. Lett. **101**, 151802 (2008).

[22] A. Anastassov *et al.* [CLEO Collaboration], Phys. Rev. Lett. **82**, 286 (1999).

[23] S. B. Athar *et al.* [CLEO Collaboration], Phys. Rev. D **73**, 032001 (2006).

[24] B. Auber et al [BABAR Collaboration], Phys. Rev. Lett. **103**, 081803 (2009).

[25] M. Bartsch, M. Beylich, G. Buchalla and D. N. Gao, JHEP **0911**, 011 (2009).

[26] K. F. Chen *et al.* [BELLE Collaboration], Phys. Rev. Lett. **99**, 221802 (2007).

[27] A. J. Buras, Acta Phys. Polon. B **41**, 2487 (2010).

[28] The CMS and LHCb Collaborations, LHCb-CONF-2011- 047, CMS PAS BPH-11-019.

[29] I. Low, P. Schwaller, G. Shaughnessy and C. E. M. Wagner, arXiv:1110.4405 [hep-ph]. Note that in deriving the constraint on the invisible width of the simplest singlet dark-matter model, the authors have used the ATLAS and CMS older analysis available at that time. Using the latest analysis [12, 13] will rule out the possibility of opening up the Higgs window above 140GeV in the one singlet model.